Proceedings of ICRC 2001: 692 © Copernicus Gesellschaft 2001

ICRC 2001

On the light signals in the fluorescent detector of the Pierre Auger Observatory.

M. Giller, J. L. Kacperski, W. Tkaczyk, and G. Wieczorek
Division of Experimental Physics, University of Lodz, Poland

Abstract. The analysis of fluorescence light, emitted by the atmosphere when an extensive air shower passes through it, serves as a method of detection of high energy cosmic rays. The accuracy of the determination of the primary energy depends on the proper reconstruction of the cascade curve (the number of charged particles varying with atmospheric depth). To this end it is necessary to detect an unbiased fluorescence image of the shower. Here we have studied the effect of the shower lateral distribution on the image formed in the fluorescence detector (FD) with angular resolution 1.5° and PMT sensitivity as that in the Auger experiment. We have also calculated time profile of the light signals in individual pixels (PMTs) and the influence of the finite shower disk thickness and its curvature on signal shapes. Calculations include the spherical aberration effect blurring the image. We show that quite often a non-negligible part of the signal may be hidden in the 'side' pixels.

1 Introduction

The image of an extensive air shower in the fluorescent light (integrated over time) is a narrow track on the sky, corresponding to an aligned sequence of hit PMTs (pixels) of the FD camera. In order to determine the primary energy of a shower correctly it is necessary to detect as much of the emitted light as possible. In this paper we shall try to find answers to several questions which could be important in the shower reconstruction process. These are:

- what fraction of the light signal from a certain level of the shower development (mainly at shower maximum) falls on the side pixels, and in what conditions they would not trigger?

- what are the time profiles of the light signals and is a finite shower disk thickness and its curvature relevant?

- to what extent does the spherical aberration change the above characteristics?

Correspondence to: M.Giller (mgiller@kfd2.fic.uni.lodz.pl)

2 Shower track width integrated over time.

The finite width of a shower image is a result of the lateral spread of the particles, conventionally described by the Nishimura-Kamata-Greisen (NKG) function:

$$f(r) \sim \left(\frac{r}{\mathrm{r}_M}\right)^{s-2} \cdot \left(1+\frac{r}{\mathrm{r}_M}\right)^{s-4.5} \quad (1)$$

where *s* is the shower age parameter (*s* = 1 for shower maximum) and $\mathrm{r}_M = \frac{21MeV}{\mathrm{E}_{cr}} \cdot \mathrm{x}_0$ is the Moliere radius, E_{cr} is the critical energy, x_0 - the cascade unit of the air.

If the image of the shower axis passes through the center of a pixel (central pixel), the number of particles seen (being proportional to the number of collected photons) is that contained within a strip centered on the axis, with its width equal to the product of the pixel angular size (1.5°) and distance to the shower.

Since the NKG function for a given *s* depends on the dimensionless distance $x = r/\mathrm{r}_M$ only, one can calculate a universal curve giving the fraction of the total number of particles seen by the central pixel. The results are presented in Fig. 1. It can be seen that at the shower maximum about 93% of particles are contained within the $2 \cdot \mathrm{r}_M$ strip, 50% being within $2{\cdot}0.15\mathrm{r}_M$. Vertical lines show the central pixel field of view and are drawn for $\mathrm{r}_M = 140m$, the value corresponding to the height in the atmosphere where proton initiated showers with $\mathrm{E}_0 = 10^{20}eV$ and zenith angle 45° have their maxima. For *s* = 1 and distances 5, 10 and 20 km the fractions outside the central pixel are 19, 7 and 2% respectively. Below the maximum they become larger.

So far, we have neglected the spherical aberration of the mirror. This effect causes a parallel beam of light incident on the spherical mirror to form a spot of a finite size on the focal surface. An analytical solution for the spot size has been found [1] by us. For the Auger FD the diameter of the spot comes out to be 0.50°, which coincides with the value obtained earlier numerically [2]. To take into account the spherical aberration we shall assume that the light intensity

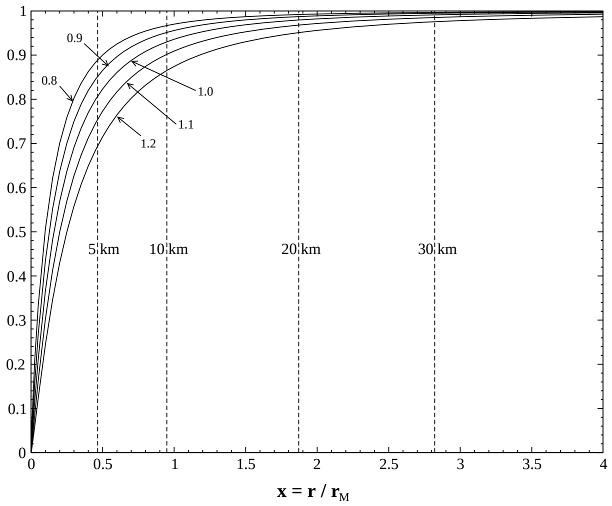

Fig. 1. Fraction of particles contained within strip *2x* for the NKG lateral distribution for several values of *s*. Dashed vertical lines correspond to fields of view of the central pixel for showers 5, 10, 20 and 30 km away, for $\mathrm{r}_M = 140m$. No spherical aberration.

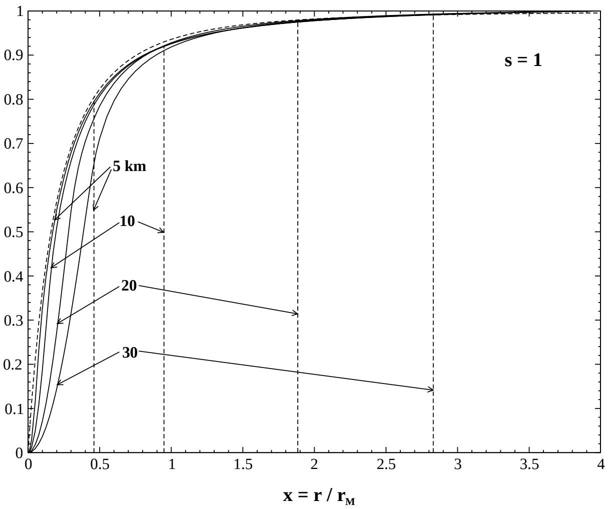

Fig. 2. Fraction of particles (light) contained within strip *2x*, for the lateral distribution *f'(x)*, where spherical aberration has been allowed for. Dashed line - for NKG without aberration.

across the spot is uniform (for a constant intensity in the incident beam). It is not quite true for a perfect spherical mirror [3], but real mirror imperfections smooth to some extent the intensity profile. As the spherical aberration smears the image, allowing for it is equivalent to modifying (smearing) the lateral distribution of particles and leaving the mirror without aberration. The modified lateral distribution function $f'(r)$ can then be calculated from the formula:

$$f'(r) = \int \frac{f(r') \cdot ds(r')}{\pi \rho^2} \tag{2}$$

where ρ is the smearing radius, equal to $0.25° \times$ distance to the shower, *r'* is the core distance and *ds(r')* is the surface of the ring element *(r', r'+dr')* contained within the circle of radius ρ with the center at core distance *r*. The integration is carried out over the whole surface of this circle and the results for *s* = 1 are presented in Fig. 2. As it should be expected, the larger is the distance to the shower, the bigger is the difference between the modified and the NKG functions. The calculations were done for distances *l* = 5, 10, 20 and 30 km. Although the distribution of light within the pixel is changed, the total fraction of light within it remains practically unchanged for any *l*. For smaller *s* the effect is bigger.

3 Time dependence of the signals.

Now we shall investigate the time evolution of the light flux arriving at a particular pixel. As it has already been explained [4] the instantaneous image of a shower has circular symmetry which results from the axially symmetrical lateral distribution of the particles. If the angle between the shower axis and the line of sight is θ, then photons arriving simultaneously at a pixel would have been produced by particles while crossing a plane inclined at angle $\theta/2$ to the shower axis.

As time progresses the plane moves away from the detector. In other words, a pixel sees the light from the plane moving away from the detector with the light velocity *c* along the line of sight. Thus, the time profile of the light flux falling on a given pixel reflects directly the variation of the number of particles on that plane 'cut-out' by the pixel's field of view.

Fig. 3 represent the results of the calculations. Flux time profiles are shown for pixels seeing a shower perpendicularly to the axis for distances *l* = 5, 10 and 20 km, at the age parameter *s* = 1. On each graph there are three sets of curves corresponding to three pixels numbered 1, 2 and 3, located perpendicularly to the shower axis crossing the center of pixel 1. Thus the angular distance of the center of pixel 2 (3) from the shower axis is $1.5°$ $(3°)$. For each pixel there are drawn three curves. The solid line describes the signal time profile for an infinitely thin shower disk (a plane) with no spherical aberration taken into account. The dotted line allows for the aberration. Additionally, considering finite thickness of the shower disk, we obtain the dashed curve. Here we assumed that particle density at a given instant changes as a Gaussian function along the line perpendicular to the disk, with $\sigma = 30$ m (100 ns), the modified NKG density at this distance being the integral over the Gaussian distribution. Such a shower disk is just a sum of many thin disks entering pixel's field of view with increasing time delays. The actual numbers on the vertical axis are the fractions of all shower particles at a given level seen by the pixel at a given time. Time *t* = 0 corresponds to the shower core crossing the center of pixel 1.

Inspection of Fig. 3 leads to the conclusions:

- The signal maximum in pixel 2 can reach several percent

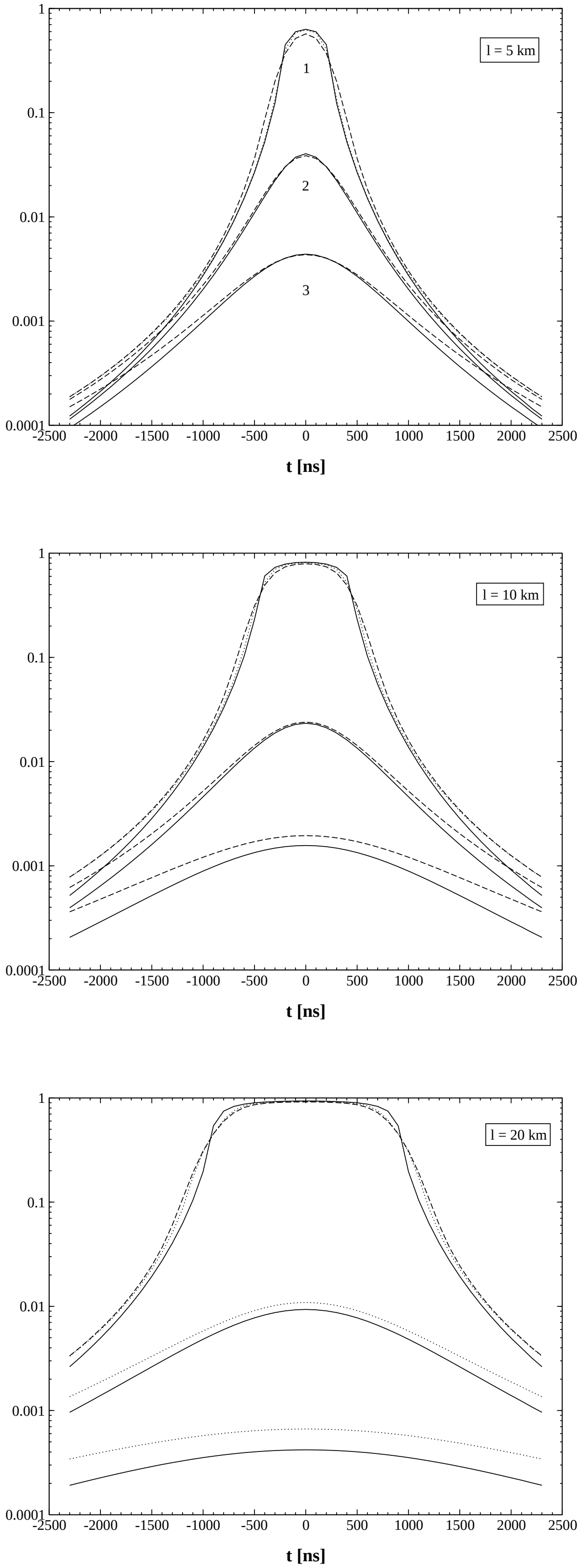

Fig. 3. Time shapes of light fluxes (time in ns) from shower maximum (*s* = 1) at three lateral pixels (see text). Solid lines - NKG lateral spread only, dotted lines - aberration allowed for, dashed lines - finite disk thickness ($\sigma = 30$ m) additionally included.

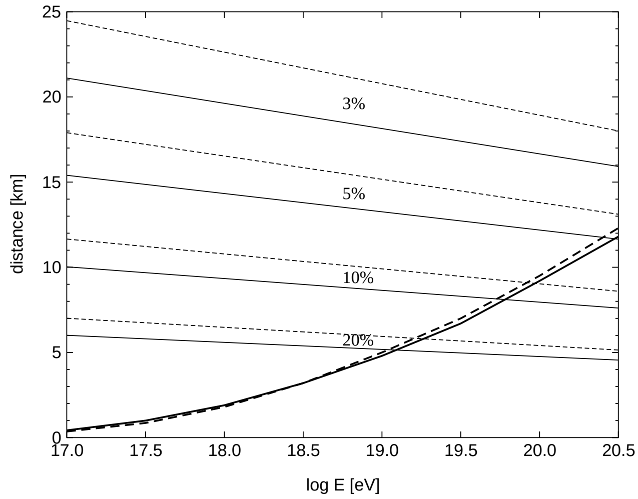

Fig. 4. Distance to the shower maximum (rising lines), above which the peak value of the signal in the first side pixel (pixel 2) drops below 4σ of the background, vs primary energy of a proton (solid line) and iron nucleus (dashed line) for zenith angle $\theta_z = 45°$. Falling curves show distances at which the signal in both side pixels integrated over time is 3, 5, 10 and 20% of the total at this level.

of that in pixel 1, if distance *l* to the shower is smaller than 10 km; for pixel 3 it is below 1%, even for *l* = 5 km. However, as the shower line would go close to a pixel center rather rarely, these fractions should be treated as lower limits.

- The spherical aberration becomes important for $l > 10$ km; (for smaller *s* the effect is always more significant than that for bigger because of a steeper lateral distribution). The smoothing of the trapezoidal shape is significant for $l \geq 20$ km; for smaller distances the shapes are far from trapezoidal.

- The effect of a finite disk thickness can only be important for steep signal slopes, i.e. for small distances. It is not clear what this thickness is for big showers near the axes, but our calculations show that this effect would be important for $l \leq 5$ km only, if $\sigma \geq 30$ m.

The shapes of the signals in the two side pixels (2 and 3) could actually be deduced from that in the central one, due to the circular symmetry of the disk image, when the shower axis crosses the center of pixel 1. For example the signal maximum in pixel 2 should be equal to the value corresponding to $t = \pm 1.5° \cdot l/c$ for pixel 1 (we assumed that the pixel field of view is circular, with the solid angle the same as that for the hexagon with $1.5°$ side to side).

The time scale in Fig. 3 is appropriate for the line of sight perpendicular to the shower axis ($\theta = 90°$). For another angle θ one has to multiply the time scale by $1 - \cos\theta$, meaning that its change is the biggest at $\theta = 90°$.

The results presented so far do not depend on the primary energy of a shower, if the shape of the lateral distribution function depends on the age parameter *s* only. (Actually, it does depend to some extent on the primary energy because the most representative value of the Moliere radius r_M should be larger for smaller energies). However, we would like to investigate now how much of the light flux would be hidden in the side pixels which have not been fired and this, of course, depends on absolute light fluxes and, therefore, on primary energy. For an adopted level of the background light one can find the minimum distance *l* to the maximum of a shower with a given energy when the side pixels remain inactive. Here, we assume for the background level 50 photoelectrons (pe) emitted from the PMT cathode per 100 ns, and for the trigger threshold 4 standard deviations (~ 28 pe) above the background. Each charged particle causes an isotropic emission of 4.5 photons per 1m of its track. For the attenuation length we adopt $\lambda = 8.4$ km and the rest of the necessary parameters are appropriate for the FD: mirror diaphragm area - 1.5 m^2, its reflectivity - 0.9, photocathode efficiency - 0.3.

Number of charged particles at shower maximum and its depth in the atmosphere have been taken from Pryke [5] (as averages from the four interaction models considered there). Rising lines in Fig. 4 show the calculated distance to the shower maximum, above which the maximum value of the signal in the first side pixel (pixel 2) drops below 4σ of the adopted background level, as a function of primary energy of a proton (solid line) and an iron nucleus (dashed line). Falling curves show distances at which the signal in the side pixels integrated over time is 3, 5, 10 and 20% of the total at this level. These distances decrease with energy only because of different Moliere radii adopted for different energies. Comparing these curves with the rising lines it can be seen that e.g. for proton showers with $E \approx 10^{20} eV$ up to 8% of the signal (at *s* = 1) would not fire the side pixels, if $l \geq 10$ km. At $\sim 10^{19} eV$ it is $\leq 20\%$, with distances $\geq 5km$. For iron showers these fractions become larger.

4 Shower disk curvature and its image.

A question may arise to what extent a curvature of the shower disk can change its instantaneous image, i.e. our results obtained so far. Of course, this effect should not be as important for the fluorescent image of a shower as it is for its ground characteristics, where arrival times of particles are measured over distances of several kilometres. Here we are interested in the curvature effect up to the core distances of $r \leq 200$ m or so. The situation is illustrated in Fig. 5. We have assumed that the shower disk is a thin plane. For its particular shape we have taken simulation results of Sciutto [6] for the electron mean delay time as a function of the distance from the shower core, for $E = 10^{20.5}$ eV (primary proton). It has been drawn in scale as a solid line in Fig. 5 where the ordinate coincides with the shower axis. When its image crosses the center of a pixel, the distance ranges seen from 10 km by the central and both side pixels would be those marked by the vertical dashed lines. For this particular configuration the particles seen by the central pixel would be delayed by less than $\sim 50ns$ with respect to those on the axis. We have additionally drawn a curve from Fig. 1 (the thinner line with the scale on the right hand side) showing the fraction *F* of all particles on this level ($s = 1$) within strip *2r*. The

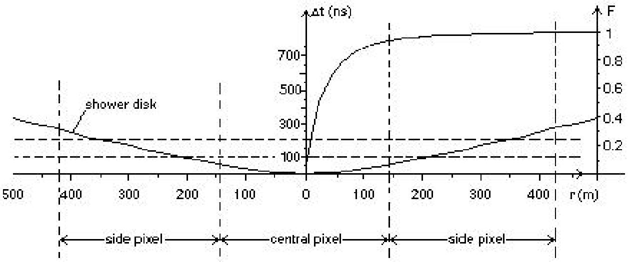

Fig. 5. Intersection of a shower disk with a plane containing the axis. Fraction *F* of light, contained within strip *2r* for $s = 1$, has been marked by the thinner line (the right vertical axis). Also pixel fields of view from 10 km are shown.

time spread due to disk curvature in the side pixels is bigger ($\sim 200ns$) but only about 3% of all particles on this level would be delayed by more than 100 ns.

5 Conclusions.

In this paper we have been investigating to what extent the characteristics of real showers, such as lateral spread of particles or finite disk thickness and its curvature, would affect their images. Assuming that the particle lateral distribution is described well by the NKG function we have shown that side pixels may contain non-negligible fractions of the light flux, without being triggered. The actual numbers depend, of course, on the background level adopted, but it seems that it is important to look for the signal in the non-triggered side pixels in the shower reconstruction procedure.

Time profiles of the signals are not well described by trapezoidal shapes, as it is often considered: for small distances the signals are too short, for large distances - the spherical aberration smoothes the shapes.

A finite disk thickness smoothes slightly the time profiles of the signals, this effect dominating that of the aberration for $l \leq 15$ km (if $\sigma = 30m$).

Due to shower disk curvature particles distant by more than ~ 200 m from the axis (near shower maximum) would be delayed by more than 100 ns, their fraction being however a few percent only.

Acknowledgements. This work has been supported by the Polish State Committee for Scientific Research (KBN grant No. 2 P03C 006 18). The authors thank Z. Szadkowski for useful discussions.

References

[1] M.Giller, J.L.Kacperski, W.Tkaczyk and G.Wieczorek (in preparation)
[2] P.Sommers (private communication)
[3] G.Matthiae and P.Privitera, *GAP-98-039*
[4] P.Sommers, *Astroparticle Physics* 3 (1995) 349
[5] C.Pryke, *GAP-98-035*
[6] S.Sciutto (private communication)